Journal of Photochemistry and Photobiology A: Chemistry 205 (2009) 129–138

Contents lists available at ScienceDirect

Journal of Photochemistry and Photobiology A: Chemistry

journal homepage: www.elsevier.com/locate/jphotochem

Spectra and dynamics of an ionic styryl dye in reverse micelles

D. Sahoo, S. Chakravorti*

Department of Spectroscopy, Indian Association for the Cultivation of Science, Jadavpur, Kolkata 700032, India

ARTICLE INFO

Article history:
Received 29 December 2008
Received in revised form 6 April 2009
Accepted 22 April 2009
Available online 3 May 2009

Keywords:
Reverse micelle
TICT
Micropolarity
Microviscosity
Quenching

ABSTRACT

The interesting influence on the photophysics of an intramolecular donor–acceptor system 2-(4-(dimethylamino) styryl)-1-methylpyridinium iodide (DASPMI), a known selectively staining agent of mitochondria in living cells, by the monodispersed biomimicking nanocavities formed by the anionic sodium 1,4-bis-2-ethylhexylsulfosuccinate (AOT)/n-heptane and the cationic benzyl-n-hexadecyl dimethylammonium chloride (BHDC)/benzene reverse micelles and also water-in-oil (n-heptane/(AOT)/water or benzene/(BHDC)/water) have been reported in this paper. Red shift of DASPMI emission in AOT with increasing water pool size ($W = [H_2O]/[surfactant]$) indicates that the probe molecule moves towards core and the blue shift in BHDC in the same condition is indicative of the probe remaining away from the core. The partition constant K_p in two RMs correlate well with the position of emitting probe DASPMI in RMs interface and it corresponds nicely with the values obtained from anisotropy data. Reduced quantum yield of TICT emission with increasing pool size (W) in AOT due to non-radiative decay through hydrogen bonding suggests that the acceptor group is at the interface directed towards water pool. In AOT decreasing anisotropy along with active non-radiative channel confirm the presence of the probe at the water/AOT interface. The rotational restriction experienced by DASPMI in anionic reverse micelle decreases with increasing hydration. The in situ measurements of micropolarity and microviscosity around the probe with increasing W show enhanced micropolarity and a decrease in microviscosity. Increased emission quenching by Cu^{2+} is due to counterion exchange of Cu^{2+} by Na^+ at the micellar interface and due to increased local concentration of Cu^{2+}. It again confirms that the probe molecule does not penetrate into the core rather it binds at the interfacial region. The unaffected TICT emission in fluorescence quenching study in BHDC confirms position of probe away from the core.

1. Introduction

Reverse micelles (RMs) are water-in-oil droplets stabilized by surfactant molecules in hydrocarbon solvents with charged groups pointing inwards and the tails in the bulk solvent [1] could be used to control the extent of confinement symmetrically. The polarity, viscosity and hydrogen bonding ability of water inside pool and confined at the interface vary [2] with pool size W ($W = [H_2O]/[surfactant]$). High ionic strength and a heterogeneous micropolarity [1–4] are associated with interfacial region. It was established from previous studies [5] of solutes in water pool that water pool is less polar and has less hydrogen bonding ability than bulk water. A layered water structure was suggested by both experimental [6–8] and modeling studies [9–11]. So that RMs can in principle be used to systematically vary the solvation characteristics and examine how the spectra and dynamics are affected. Dynamical processes in RMs often occur more slowly than in bulk water as observed previously by several time resolved studies like solvation dynamics [12–14], internal charge transfer [15–17], isomerization, dielectric relaxation [18,19] and transient infrared spectroscopy [20,21]. The RMs can be made by using cationic, anionic, or non-ionic surfactants. The correlation between spectral shifts and dynamics of the probe species with the surfactant charge, specially charged solute species [12,13] are well reported facts relating to the location of the probe within the RMs interior and also how it depends on the surfactant charge.

Quest for an appropriate mechanism for biological and chemical energy conversion [22–24] has spurred the proliferation of interest in photoinduced intramolecular charge transfer (ICT) of various organic molecules containing electron donor and the acceptor groups in recent times. The interesting multi-bond rotation involved TICT photophysical property [25] of ionic styryl dye 2-(4-(dimethylamino) styryl)-1-methylpyridinium iodide (DASPMI) has many applications [26,27]. The TICT photophysics of DASPMI is dependent on both polarity and microviscosity of the medium [28]. Ramadass et al. proposed excited state kinetics of DASPMI as a three-state model of LE, ICT and TICT states. Fluorescence intensity of DASPMI is a dynamic measure for the membrane potential of mitochondria [29]. In living cells, uptake of the dye is strongly influenced by inhibitors of oxidative phosphorylation such as CCCP

* Corresponding author. Fax: +91 33 2473280.
E-mail address: spsc@iacs.res.in (S. Chakravorti).

1010-6030/$ – see front matter © 2009 Elsevier B.V. All rights reserved.
doi:10.1016/j.jphotochem.2009.04.018

(carbonylcyanide-m-chlorophenylhydrazone). The quantum yield of fluorescence is influenced by polarity of the environment and the dissipation by twisted intramolecular charge transfer (TICT) is determined by the microviscosity of the environment [30]. This simultaneous dependence of styryl dye photophysics on viscosity and polarity has offered several applications in polymer science and cell biology. The dependence of photophysics of these molecules on polarity and viscosity in unison opened up the possibility of different applications [27,31,32].

Potentially useful models of the bio-environments are micelles and cyclodextrins and we have done some work, as our continuing effort, to explore these environments with probe molecule [33,34]. DASPMI is a popular and important staining agent for mitochondria and we were intrigued in using it in biomimic membrane systems—reverse micelles before moving to real life situations. The basic intention of the present study is to investigate thoroughly the photophysical property change in DASPMI embedded in reverse micelles containing the anionic surfactant sodium AOT (sodium 1,4-bis-2-ethylhexylsulfosuccinate) which has the ability to solubilize a large amount of water with values of W and also in cationic surfactant BHDC (benzyl-n-hexadecyl dimethyammonium chloride) [35] reverse micelles as well as the in situ measurement of micropolarity and microviscosity inside the RMs. Position and orientation of the probe in RMs will also be investigated.

2. Experimental

2.1. Materials

2-(4-(Dimethylamino) styryl)-1-methylpyridinium iodide (DASPMI) (Chart 1) was received from Aldrich Chemical, USA and purified by column chromatography (on silica gel 60–120; 5% ethyl acetate in petroleum ether). The purity of the compound was checked by thin layer chromatography (TLC). The compound was then vacuum sublimated before use. n-Heptane, acetonitrile (spectroscopy grade), both from Aldrich, and AOT, BHDC (ultra grade) from Sigma were used as received. The molar ratio of residual water/AOT, as determined by Karl–Fischer titration, was found to be 0.2. Millipore water was used in the preparation of water-in-oil microemulsion.

2.2. Sample preparation

A solution of DASPMI (5×10^{-5} M) was prepared in n-heptane. Binary mixtures of n-heptane/AOT were prepared by adding the required amount of AOT into 5 mL each of second stock solution. We used the stock solution containing 5×10^{-5} M dye in a binary solution of 0.1 M AOT in n-heptane for the preparation of n-heptane/AOT/water mixtures. And for different W the solution was prepared by adding appropriate amount of Millipore water, using calibrated micropipettes, to the binary stock solution. To get a homogeneous mixture we sonicated the solutions for 3–5 min. The samples were kept for 15–20 h at room temperature before carrying out all the measurements. The same method was used for preparation of BDHC solution in benzene.

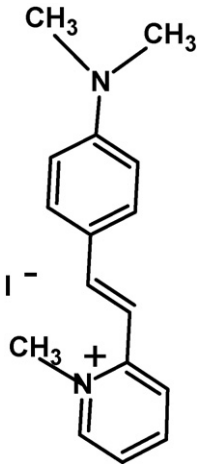

Chart 1. Structure of DASPMI.

2.3. Methods

The absorption spectra were taken with a Shimadzu UV–vis absorption spectrophotometer model UV-2401PC. The fluorescence spectra were obtained with Hitachi F-4500 fluorescence spectrophotometer. Quantum yields were determined by using secondary standard method ($\varphi_f = 0.23$) with recrystallized β-naphthol in MCH (methylcyclohexane), details of the process are described elsewhere [36,37]. For lifetime measurement the sample was excited (at 440 nm: o.d. ~0.15) with pico-second diode (IBH Nanoled-07). The time correlated single photon counting (TCSPC) set up consists of Ortec 9327, TBX-04 detector, DataStation measurement software and DSA6 Foundation Package. The data were collected with a DAQ card as a multichannel analyzer. The typical FWHM of the system response is about 80 ps. Typical slit width ~30 nm, monochromator type Jobin-Yvon, number of channels 4000 (6 ps per channel), window width ~24.5 ns and number of counts ~10,000 were used in taking decay profiles. Data analysis was carried out using the curve-fitting program supplied by the manufacturer. Quality of the fit was determined by the reduced χ^2 and a high Durbin–Watson parameter (>1.7) [38].

3. Results and discussion

3.1. Absorption and emission of DASPMI in n-heptane/AOT and benzene/BHDC reverse micelle

DASPMI in n-heptane exhibits an absorption maximum at 410 nm (Fig. 1a). Addition of AOT to an n-heptane solution DASPMI results a decrease in absorbance and hypsochromic shift of absorbance peak. For BHDC cationic reverse micelle the absorption maximum of DASPMI is also blue-shifted with the increase of reverse micelle concentration (Fig. 2a). The relative contribution of resonance hybrids of the probe, i.e., benzenoid and the quinoid forms is responsible for solvent induced polarity-dependent shift. Because of being more localized π-electrons the benzenoid form becomes more polar and makes it more favorable in polar solvents and a consequent blue shift is observed in the absorption spectrum in both the reverse micelles. Moreover the blue shift in absorption spectra along with the decrease in quantum yield in reverse micelles may be interpreted as the dissipation of energy by the formation of charge transfer state.

DASPMI in n-heptane shows an emission peak at 536 nm (Fig. 1b). With increase in concentration of AOT from 0 M to 0.2 M, a gradual blue shift in the fluorescence spectrum is observed. Changing excitation wavelength does not affect the fluorescence spectrum of DASPMI in binary mixture. The above observation of blue shift indicates that the benzenoid form of the probe molecule is sensing an increasingly polar microenvironment in both ground and excited states.

In benzene DASPMI shows an emission peak at 558 nm and with increasing the concentration of BHDC a spectral increment with blue shift is observed and finally the peak is observed at 554 nm with BHDC ~0.2 M (Fig. 2b). The hypsochromatic shift of emission maximum observed by increasing the surfactant concentration is

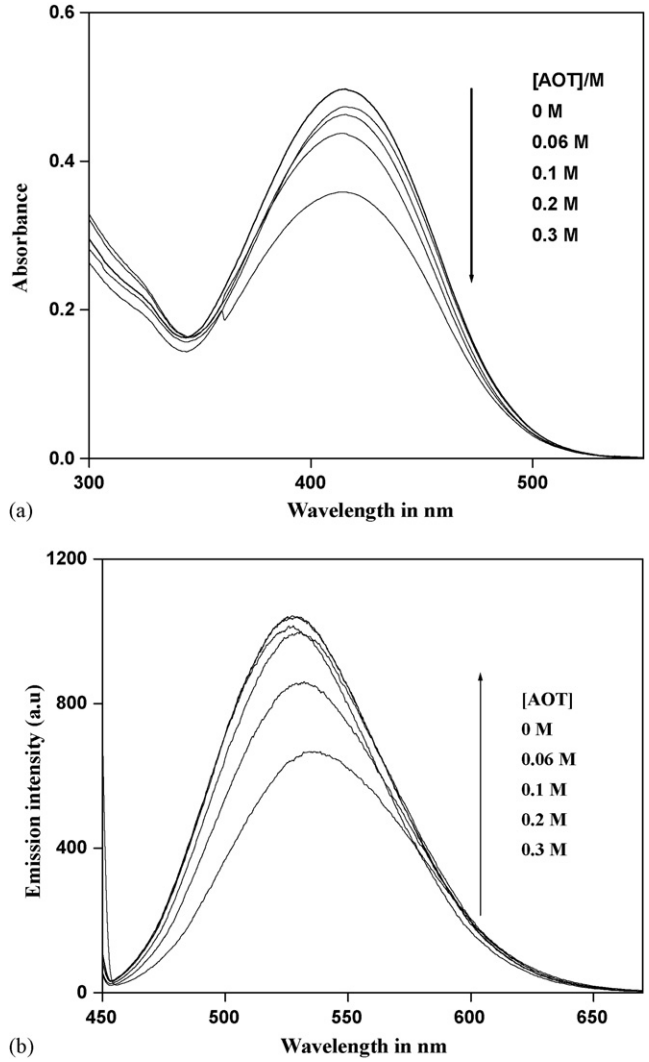

Fig. 1. (a) Absorption spectra of DASPMI at different concentrations of AOT in n-heptane/AOT solution at $W = 0$. (b) Fluorescence spectra of DASPMI at different concentrations of AOT in n-heptane/AOT solutions at $W = 0$.

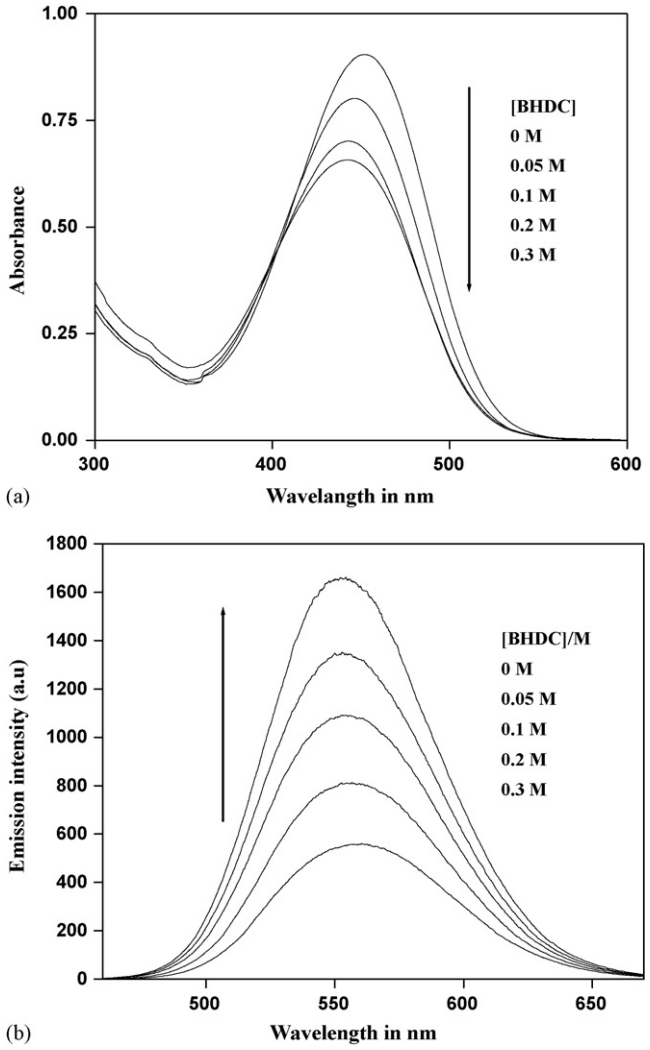

Fig. 2. (a) Absorption spectra of DASPMI at different concentrations of BHDC in benzene/BHDC solution at $W = 0$. [DASPMI] = 5×10^{-5} M. (b) Fluorescence spectra of DASPMI at different concentrations of BHDC in benzene/BHDC solutions at $W = 0$. [DASPMI] = 5×10^{-5} M.

due to the higher polarity sensed by DASPMI when aggregates are forming. This apparent dependence on the solubility behavior of DASPMI with the surfactant concentration is the characteristic feature of the system. For both in AOT and BHDC RMs the emission peak is blue-shifted which most probably indicates that emission is only from LE (locally excited) state. In the binary mixture DASPMI emits from locally excited state (LE) only.

3.2. Time resolved emission in AOT/n-heptane and BHDC/benzene

The fluorescence lifetime of DASPMI in the range of 0.03 M and 0.1 M AOT concentration monitored at 560 nm is shown in Table 1. The decay of DASPMI (excitation at 440 nm) in AOT/n-heptane binary solution can be fitted as bi-exponential functions with time constants 970 ps and 1750 ps. The contribution of shorter lifetime (τ_1) is due to the fluorescence lifetime of DASPMI in n-heptane and longer component (τ_2) corresponds to the probe in the AOT reverse micelle (RMs) interface. Also for cationic micelle (BHDC) the emission is fitted to double exponential decay and with increase of micellar concentration the contribution for reverse micelle is increased.

The above observation suggests that at higher AOT concentrations both the non-polar solvent phase and the micellar (RMs) phase are being sensed by the dye. In the absence of ionic interaction, the driving force in the form of hydrophobic interaction between the dye and hydrophobic tail of AOT possibly helps to associate the dye in the micellar phase. Apart from hydrophobic force, the dipole–dipole interaction [39,40] also comes into play as the

Table 1
Fluorescence lifetime (τ) of DASPMI in AOT/n-heptane and BHDC/benzene[a].

Concentration in M	In AOT				In BHDC			
	a_1	τ_1 (ps)	a_2	τ_2 (ps)	a_1	τ_1 (ps)	a_2	τ_2 (ps)
0.03	0.82	970	0.18	1750	0.80	990	0.20	1775
0.1	0.78	980	0.22	1900	0.75	975	0.25	2025

[a] [DASPMI] = 5×10^{-5}.

electron donor (dimethylamino) group of DASPMI may expected to be aligned close to polar head group of the surfactant. Consequently this can lead to the presence of dye molecules in the interface of the reverse micelles. For BHDC the hydrophobic interaction is same as that of AOT, but the electron donor (dimethylamino) group of DASPMI may be expected to be aligned far from the positive polar head of the surfactant.

The pseudophase model [41] which considers only changing W value in reverse micelles and independent of AOT concentration was invoked while measuring the partition function (K_p) of DASPMI between the AOT or BHDC RMs and the external solvent. Considering two solubilization sites, one the external solvent pseudophase and other the RMs interface, i.e., the distribution of DASPMI between the micelles and external solvent the partition function (K_p) of DASPMI can be determined from the following relation

$$K_p = \frac{[\text{DASPMI}]_b}{[\text{DASPMI}]_f[\text{Surf}]} \quad \text{(i)}$$

where $[\text{DASPMI}]_b$ is the analytical concentration of the substrate incorporated in the RMs, $[\text{DASPMI}]_f$ is the concentration of substrate in the organic solvent, and [Surf] is the micellized surfactant (total AOT concentration minus the 'operational CMC' $\approx 10^{-4}$ M obtained using the absorption or emission bands shift with the AOT concentration of different molecular probes at different water contents) [42,43]. This relation is applicable at a fixed value of W and at probe analytical concentration $[\text{DASPMI}]_T \ll [\text{Surf}]$.

From the fluorescence intensity change of the probe with the surfactant concentration at a given wavelength we can measure the value of K_p. If the analytical concentration of the probe is kept constant and the absorbance of the sample at the working excitation wavelength is low we arrive at the following equation [44]

$$I = \frac{I_0(\varphi_f + \varphi_b K_p[\text{Surf}])}{1 + K_p[\text{Surf}]} \quad \text{(ii)}$$

where I_0 is the incident light, I is the fluorescence intensity measured at the surfactant concentration considered (0.3 M), and φ_f and φ_b are the fluorescence quantum yields of DASPMI in the organic solvent and bound to the RMs interface, respectively.

As the concentration of RMs is increased the steady state fluorescence anisotropy increases which indicates that the probe senses a higher microviscosity inside the RMs pseudophase than that in the bulk solvent. The relationship between steady state anisotropy $\langle r \rangle$ and the surfactant concentration as obtained from the additive law of anisotropy [45] gives us the value of K_p

$$\langle r \rangle = \frac{\langle r_f \rangle + \langle r_b \rangle K_P[\text{Surf}]}{1 + K_P[\text{Surf}]} \quad \text{(iii)}$$

where $\langle r \rangle$ is the anisotropy of the mixture (steady state), $\langle r_f \rangle$ and $\langle r_b \rangle$ are the anisotropies of the free and bound DASPMI species, respectively, $[\text{DASPMI}]_T$ is the analytical probe concentration.

The values of K_p in both the RMs (Table 2) are in good agreement between the values obtained from the emission and anisotropy data. It is interesting to observe that the value of K_p in BHDC/benzene is slightly higher than that in AOT/n-heptane RMs which may be attributed to greater specific interaction between the cationic polar head of the surfactant and the probe through aromatic π-electron cloud. This specific interaction is an effective driving force for the molecular probe to reach the cationic RMs interface.

Table 2
Equilibrium constants (K_p) for partition function of DASPMI in AOT and BHDC reverse micelles as a function of W.

W	In AOT		In BHDC	
	K_P^{Em} (M^{-1})[a]	K_P^{An} (M^{-1})[b]	K_P^{Em} (M^{-1})[a]	K_P^{An} (M^{-1})[b]
0	11.5 ± 0.6	10.3 ± 0.5	12.5 ± 0.2	13 ± 0.4
10	12 ± 0.2		14 ± 0.5	
16	15 ± 0.1		16 ± 0.1	

[a] Eq. (ii).
[b] Eq. (iii).

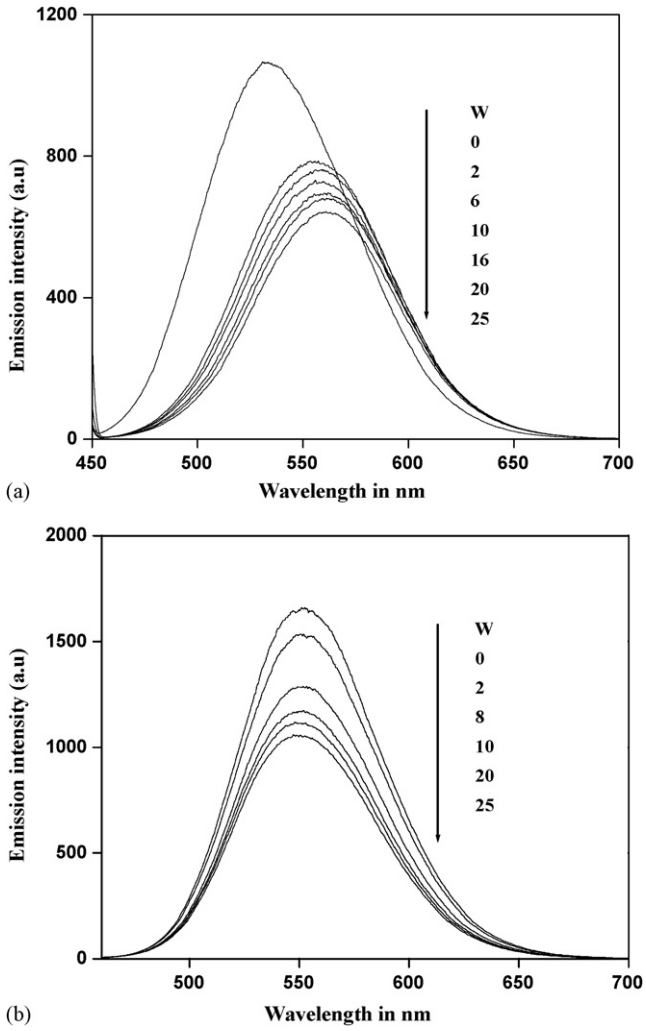

Fig. 3. (a) Fluorescence emission spectra of DASPMI at different values of W in AOT reverse micelles concentration of [AOT] = 0.1 M. (b) Fluorescence emission spectra of DASPMI at different values of W in BHDC reverse micelles. [BHDC] = 0.1 M. $[\text{DASPMI}] = 5 \times 10^{-5}$ M.

3.3. Emission of DASPMI in n-heptane/AOT/water and benzene/BHDC/water

Upon increasing the water content the pool size swells and the polarity of the microenvironments increases [46,47] resulting in red-shifted emission maximum (Fig. 3a). In the present case for anionic RMs (0.1 M AOT), as we go from $W = 0$ to higher W ($W = [H_2O]/[\text{AOT}]$) values, the emission maximum goes towards red as compared to that in n-heptane. The observation reflects that the microenvironment around the probe gets modified as we move from lower W to higher W. In such a microemulsion of $W = 25$, DASPMI exhibits red-shifted emission maximum at 562 nm compared to that in n-heptane but this value of emission maximum seems to be blue-shifted by about 13 nm from that of DASPMI in water (575 nm). The observation of blue-shifted emission maximum in the reverse micellar environments compared to that of bulk water is quite indicative of significantly differ-

Table 3
Radiative and non-radiative rate constants of DASPMI in AOT reverse micelles as a function of *W*.

W	φ_f	$K_r \times 10^{-8}$ (s^{-1})	$K_{nr} \times 10^{-8}$ (s^{-1})
0	0.62	5.7	3.5
2	0.45	3.8	4.6
4	0.43	3.4	4.7
6	0.41	3.2	4.8
8	0.39	3.1	4.85
10	0.38	2.9	4.9
12	0.37	2.8	4.95
16	0.35	2.6	5.0
20	0.34	2.5	5.0
Water	0.018	0.21	11.69

ent environment around DASPMI compared to bulk water. The shift in emission maximum due to the change in polarity experienced in anisotropic assemblies depends on the position (location) of the probe molecule. Kelker and Chattopadhyay [48] explained this issue using anthroloxy probes of different chain length and showed that the shift in the emission maximum decreases as the distance of the fluorophore increases from the water pool. Using 7-nitrobenz-2oxa-1,3 diazol-4-yl (NBD)-cholesterol they found that the emission maxima were invariant with increased *W* number, indicating that the probe molecule is located in a region far from the water pool of the RMs. In our present work the emission maximum is sensitive to *W* up to a certain level, so following Kelker and Chattopadhyay [48] we can easily rule out the possibility of the location of the probe molecule to be in a region far from the reverse micellar core. The noticeable difference in the emission maximum in RMs and bulk water indicates that the probe molecule does not reside (or only a part of it resides) in the core region. The spectral changes could be due to the formation of hydrogen bond between the acceptor N-CH_3 and the water molecule in reverse micelles. The fluorescence quenching of many molecules having ICT state [49] occurs due to deactivation via the internal conversion (IC) resulting from hydrogen bonding [50]. Very recently Kwok et al. [51] showed that IC de-excitation rate of HICT (hydrogen bonded ICT) state is much larger than that of ICT state and it may be mainly responsible for the reduced quantum yield of DASPMI in water (Table 3).

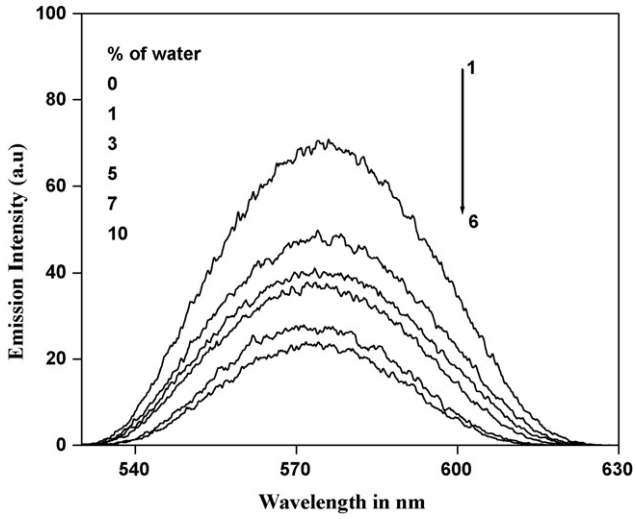

Fig. 4. Variation of emission spectra of DASPMI in acetonitrile with increase in water concentration. [DASPMI] = 5×10^{-5} M.

Thus the deactivation channel (via IC) from the hydrogen bonded ICT (HICT) of DASPMI may be responsible for the observed reduced emission in water reverse micelles.

In order to verify the hydrogen bonding effect we studied the effect of adding water in the emission spectra of DASPMI in acetonitrile solvent. As acetonitrile is a polar aprotic solvent so hydrogen bond formation between the solute and solvent is not possible. Now with addition of water in the acetonitrile solution the hydrogen bond formation between solute and solvent is possible. A sharp decrease (Fig. 4) in ICT emission spectra of DASPMI with the increase of water concentration is observed. So this observation confirms the involvement of hydrogen bonded ICT state of DASPMI in the case of reverse micelles. It has been already predicted (vide supra) that the probe molecules are located at the interface of the reverse micelles. On the basis of the hydrogen bonding between the acceptor group of the probe molecule and co-solvents for observed ICT behavior in reverse micelles we can very well predict that the probe molecules

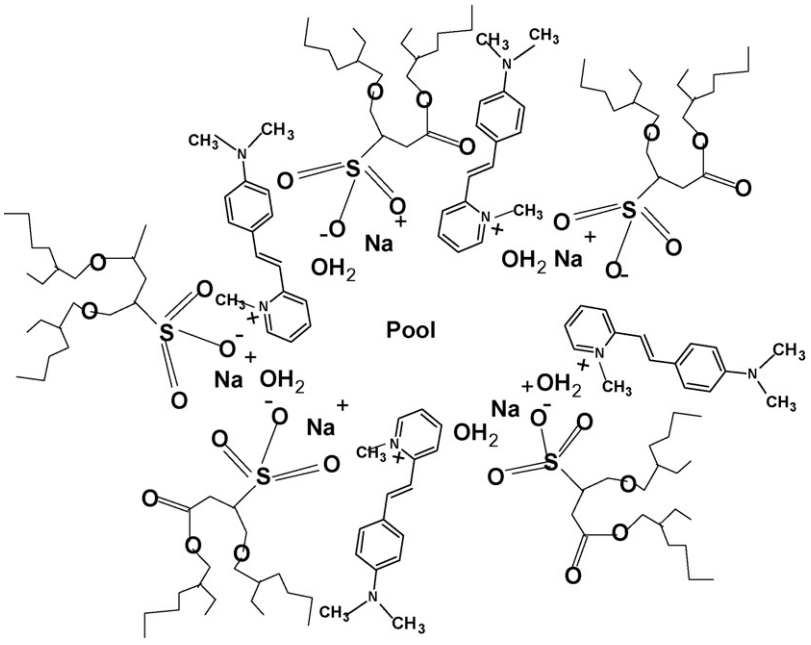

Scheme 1. Approximate presentation of orientation of DASPMI within AOT–n-heptane reverse micelle.

are oriented at the interface of reverse micelles with acceptor group towards the water pool while $-NMe_2$ group remains buried at the interface (Scheme 1).

In the case of cationic micelle (BHDC), having micellar concentration 0.1 M the emission peak is observed at 552 nm (Fig. 3b). As we go from $W = 0$ to higher W values the emission maximum decreases and moves slightly towards blue. Normally TICT emission is very much dependent on polarity of the medium and the TICT emission moves towards blue as the polarity decreases due to upward movement of TICT state. This will consequently decrease the population in the TICT state and thereby a decrease in observed emission intensity with increase in W. This strongly suggests that the probe goes far from the core (polar) region as the hydration increases.

3.4. Steady state fluorescence anisotropy

The fluorescence anisotropy indicates the extent of restriction imposed by the microenvironment on the dynamical properties of the probe. As any factor that affects size, shape, or segmental flexibility of molecule will be reflected in the observed anisotropy [48] so the measurement of fluorescence anisotropy has an important role for its tremendous potential in biochemical research. The steady state fluorescence anisotropy (r) was calculated using the relation given below

$$r = \frac{I_{VV} - GI_{VH}}{I_{VV} + 2GI_{VH}},$$

where G is the correction factor for detector sensitivity to the polarizer direction of emission and I_{VV} and I_{VH} represent the vertically and horizontally polarized emission intensity obtained on excitation with vertically polarized light.

The variation of fluorescence anisotropy of DASPMI in AOT reverse micelle as a function of water pool size W is shown in Fig. 5a suggests that the probe molecule experiences freedom in motion with bigger pool size. We also observe here that the value of r decreases rapidly until $W = 16$ and after that it levels off gradually. It is a known fact [52] that the water relaxation rate in reverse micelles is faster with the increase of W. The reduced anisotropy for the probe in the reverse micellar interface and water pool suggests the increased reorientation rate. At highest W ($W = 25$) the value of anisotropy ($r = 0.1$) is still higher than the anisotropy in pure water ($r = 0.04$, nearly isotropic), which indicates that the probe molecule in RMs still experiences a reasonable restriction compared to the situation in the bulk water. The above observations point that the probe molecule may be situated at the water/surfactant interface of the AOT reverse micelles. For cationic reverse micelles (BHDC) the anisotropy increases slightly as we increase the value of W (Fig. 5b), which possibly indicates that the probe molecule moves far away from the water core as the pool size increases.

3.5. Micropolarity around the fluorophore

Due to the great importance of the in situ determination of microscopic polarity of biological system using fluorescence probes attention has been drawn for the past few decades in this direction. The micropolarity of a biological system like protein, membrane and reverse micelles can be estimated by comparison of spectral properties of a fluorophore in that environment with those of the probe in solvents of known polarity [37,53–55]. The empirical solvent polarity parameter, $E_T(30)$ based on transition energy for the solvatochromatic intramolecular charge transfer absorption of the betaine dye 2,6-diphenyl-4-(2,4,6 triphenyl-1-pyridono) phenolate as developed by Reichardt, was used [56] to get a quantitative measure of the polarity of the local environment of DASPMI in reverse micelles taking advantage of polarity-sensitive fluorescence property of DASPMI. We have determined the micropolarity around the probe in the reverse micelles with various W values in terms of fluorescence maximum of DASPMI from the calibration plot of emission maxima of DASPMI versus known values of $E_T(30)$ (Fig. 6). Though only 78% of the probe is incorporated inside the micelle with the AOT concentration used (0.3 M) we thought of getting an in situ estimate of the micro-properties here in the line of method described [57]. Fig. 7 shows the variation of micropolarity of DASPMI in reverse micellar environments as a function of W. Fig. 7 clearly shows that with increasing W, $E_T(30)$ increases rapidly until $W = 16$ and levels off beyond that. At the highest W ($W = 25$), the $E_T(30)$ value is 53, indicating that the average environment of the probe molecule is still less polar than that of bulk water which vindicates our earlier inference from steady state fluorescence anisotropy study that the probe resides at the water–surfactant interface.

On the other hand for BHDC reverse micelles $E_T(30)$ varies very little and its overall values decrease as W increases gradually (inset Fig. 7). So the decrease in polarity indicates that the probe molecule goes far from the micellar core as the pool size increases and after a limit it eventually remains the same, which indicates that further translation does not occur even if we increase the pool size.

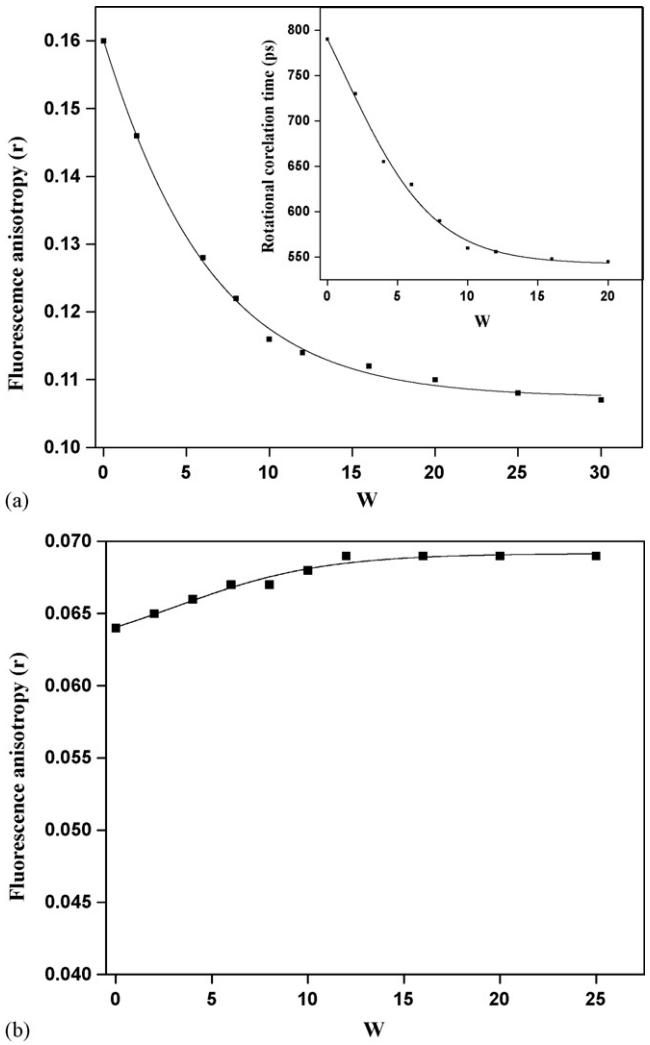

Fig. 5. (a) Steady state fluorescence anisotropy of DASPMI plotted against W in AOT reverse micelles at room temperature. Inset shows the variation of rotational correlation time as a function of W. (b) Steady state fluorescence anisotropy of DASPMI plotted against W in BHDC reverse micelles at room temperature. [DASPMI] = 5×10^{-5} M.

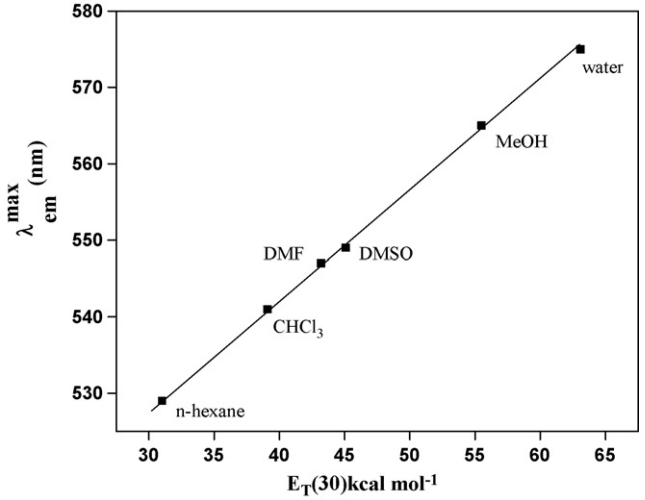

Fig. 6. Variation of emission maximum of DASPMI in different solvents as a function of $E_T(30)$.

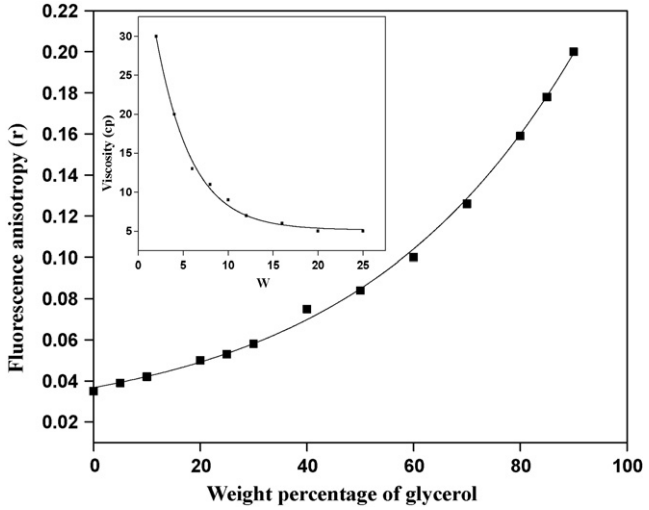

Fig. 8. Variation of fluorescence anisotropy as a function of composition of glycerol–water mixture. Inset shows the variation of microviscosity of DASPMI in AOT reverse micelles plotted against *W*.

3.6. Microviscosity around the fluorophore

The viscosity around the fluorophore influences the fluorescence anisotropy. So the in situ microviscosity at a fixed temperature is often estimated by comparing the fluorescence anisotropy of a fluorophore in an environment with those of the probe in the solvents of known viscosity [58,59]. The variation of viscosity as a function of *W* in the reverse micellar environments has been measured in the usual way [59]. Glycerol and water have nearly the same polarity so the mixture of them is taken for changing viscosity of the medium without changing the polarity. Fig. 8 shows the calibration curve monitoring the fluorescence anisotropy of DASPMI in glycerol–water mixtures against the weight percentage composition of glycerol. The microviscosity (error ∼10%) is determined in the reverse micelles of different *W* and the variation is presented in the inset of Fig. 8. It is observed from Fig. 8 that the microviscosity decreases rapidly up to *W* = 16 and thereafter it gradually decreases until the solution becomes turbid above *W* = 25, because of the limit of water solubilization. The expected high viscosity at low *W* confirms that the water molecules are tightly bound to sulfonate head group of AOT. Table 4 also indicates that the microviscosity in the vicinity of water/surfactant interface is very much higher than that of in bulk water even in fully expanded state (microemulsion). Here we find that the properties of water in the reverse micelles of AOT are quite different from that of bulk water [60]. It was suggested earlier that even at high water content the apparent viscosity is 6–8 times greater than that of free water molecules [61]. In our case at the highest *W* the estimated value of microviscosity is very much close to the value reported earlier [61]. So above result confirms that we can measure the in situ microviscosity of AOT reverse micelles, particularly in the interfacial region, of different dimensions with the help of our probe DASPMI.

So the possible mechanism in the DASPMI excited state in the reverse micellar medium is the solvent relaxation where the initially excited state relaxes to a solvent relaxed state. In general medium polarity is more effective than viscosity of the medium in TICT process. So we can say that high polarity medium is favorable for TICT process and high viscosity medium is favorable for solvent relaxation process. The micropolarity increases with the water addition up to a *W* value around 16 and then remains constant.

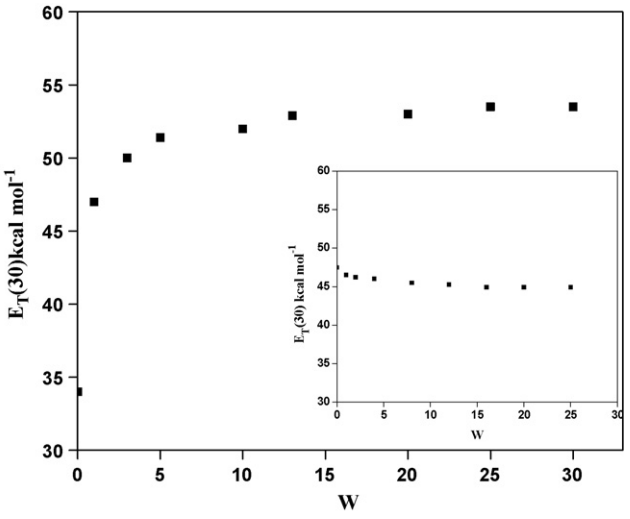

Fig. 7. Plot of $E_T(30)$ against *W* of DASPMI in AOT/n-heptane reverse micelles. Inset plot of $E_T(30)$ against *W* of DASPMI in BHDC/benzene reverse micelles.

3.7. Metal-induced fluorescence quenching

To get the probable location of the probe we have studied the quenching effect of DASPMI with the ionic quencher Cu^{2+} ($CuCl_2$) as a function of *W* and also we wanted to see how the accessibility of the probe molecule to the quencher depends on *W*. As we observed a drastic major change in position and intensity of emission of DASPMI with the gradual formation of water pool inside the AOT we

Table 4
Values of micropolarity, anisotropy and microviscosity of DASPMI as a function of *W*.

W	Emission max (nm)	$E_T(30)$ (kcal mol^{-1})	*r*	η (cp)
0	533	34	0.16	
2	552	48	0.14	27
4	555	50	0.132	20
6	558	51	0.128	13
8	559	51.8	0.122	11
10	560	52	0.116	9
12	561	52.7	0.114	7
16	562	52.9	0.112	6
20	563	53	0.11	5
25	563	53.5	0.108	5
Water	575	63.1	0.04	0.9

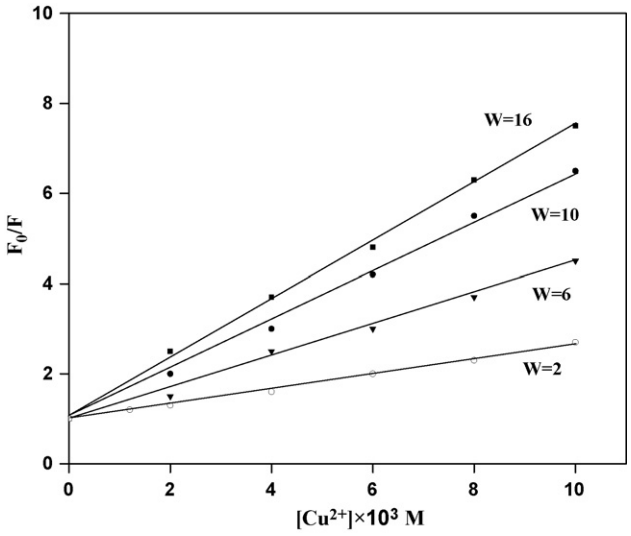

Fig. 9. Variation of relative fluorescence intensity (F_0/F) of DASPMI in AOT reverse micelles as a function of [Cu^{2+}]. [DASPMI] = 5×10^{-5} M.

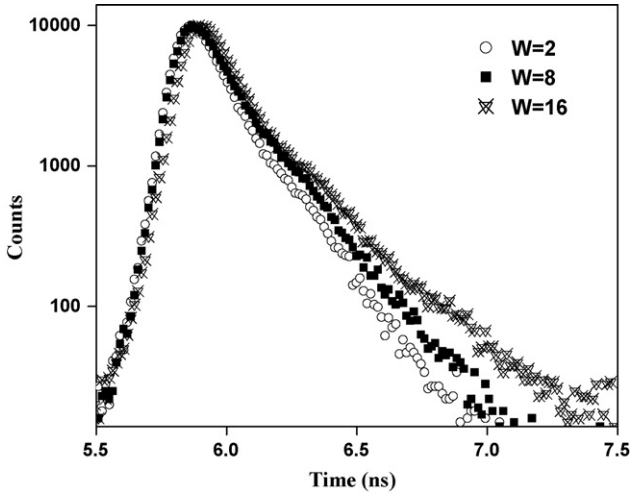

Fig. 10. Time resolved fluorescence intensity decay of DASPMI in AOT reverse micelles in different W (λ_{exc} = 440). [DASPMI] = 5×10^{-5} M.

expected all or nearly all probe molecules were within the pool and no probe molecules were present in n-heptane. With this understanding we invoked the Stern–Volmer plot of experimental results for quenching of DASPMI by Cu^{2+} in Fig. 9. The slope (K_{SV}) in the Stern–Volmer plot defines the degree of accessibility of the probe to the aqueous phase; generally higher the slope greater is the degree of accessibility [58,62]. Fig. 9 shows that the accessibility of DASPMI molecule to Cu^{2+} increases as the value of W increases and so is the increased quenching by Cu^{2+}. Any decrement of quenching process indicates the decrement of fluidity of the medium, which also slows the rate of diffusion of the interacting species. The quenching of fluorescence of different fluorophores by Cu^{2+} ion has been studied by Panda et al. [63] in aqueous and oil/water microemulsion. They showed that the relatively lower value of K_{SV} in microemulsion than water is due to interfacial barrier (by the way of solvation and separation) for the interaction of fluorophore and quencher which are populated in oil and water, respectively. So in the light of above discussion it may be concluded that the interfacial barrier and regional fluidity influence the photophysical process involving the fluorophore and the quencher. In our present case the probe is most likely to be at the interfacial region (vide supra) and the quencher Cu^{2+} (formed from the copper chloride salt inside the water pool after it overcomes the interfacial barrier) resides in the interior of water pool of the reverse micelles. So the interaction propensity is guided by both the interfacial barrier and fluidity of water inside the reverse micelles. The solvation of interfacially absorbed AOT molecules in the water pool (to the extent of 1:6 as AOT:water) [62] at low W makes the pool fluidity lower and hence reduces K_{SV}. So our results reflect that the polarity of microenvironment increases with increasing W and that also induces increased hydration. The steady state anisotropy experiment suggested that as the core size increases the probe molecule is relatively free in motion. The binding of Cu^{2+} ions with the AOT reverse micelles by displacing Na^+ (counterion exchange) at the micellar interface [64,65] is expected to increase the local concentration of the quencher around the fluorophore bound to the interfacial region within the reverse micelle which leads to an increase in the value of K_{SV}.

For cationic reverse micelle (BHDC) the quenching effect is different from AOT reverse micelles. In this case up to $W = 2$ the quenching effect is observed a little but as we increase the value of W there is practically no quenching at all (not shown). This result suggests that as we increase the value of W the probe molecule is moved from the core region gradually, which was predicted from other experiments (vide supra).

3.8. Time resolved studies of DASPMI in n-heptane/AOT/water and benzene/BHDC/water

Fluorescence lifetime acts as a sensitive parameter for exploring the local environment around a fluorophore [66,67] and it is sensitive to excited state interactions. Different extents of solvent relaxations around a fluorophore could also be expected to give rise to differences in its lifetime. In the case of DASPMI in RMs the decay becomes multi-exponential and the lifetime values are observed to be longer than in pure aqueous solution. Certainly it is difficult to extract a meaningful rate constant in such a heterogeneous system. Robinson et al. [68] pointed out that if the diffusion coefficient (D) of the probe in the water pool is the same as that of an aromatic molecule in ordinary water (0.05 Å^2 ps^{-1}) the probe molecule moves about 10 Å ns^{-1} in a direction normal to the surface ($Z^2 = 2D\langle t \rangle$). Thus the DASPMI molecule passes through several water layers within the observed lifetime of ~1 ns. The multi-exponential decay originates from the different polarity regions experienced by the molecule within its lifetime. If the diffusion coefficient inside the water pool is smaller by one order of magnitude compared to that of pure aqueous medium every DASPMI molecule would be more or less confined to one layer of water molecules. Even then there is a possibility of different DASPMI molecules in different polarity regions being excited simultaneously. That superposition of many decays of slightly different lifetimes looks like bi-exponential decays, as discussed by many workers [68,69]. In Fig. 10 the bi-exponential decay profiles of DASPMI in AOT reverse micelles are shown. In Table 5 the fluo-

Table 5
Lifetime data of DASPMI in AOT reverse micelle as a function of W.

W	a_1	τ_1 (ps)	a_2	τ_2 (ps)	$\langle\tau_f\rangle$ (ps)	τ_c (ps)
0	0.81	980	0.19	1900	1081	786
2	0.80	950	0.20	2100	1180	736
4	0.81	910	0.19	2600	1231	655
6	0.80	880	0.20	2700	1244	631
8	0.80	870	0.20	2800	1256	593
10	0.79	850	0.21	2850	1270	558
12	0.78	845	0.22	2900	1297	555
16	0.78	835	0.22	3000	1311	547
20	0.77	832	0.23	3030	1337	545
Water	0.72	600	0.28	1400	840	

rescence lifetimes of DASPMI in AOT reverse micelles obtained as a function of W are shown. A negative pre-exponential factor which is a characteristic of an excited state process should be observed in lifetime values but we could not observe the rise time of the fluorescing state because of our instrumental limitations. We have chosen the mean fluorescence lifetime defined by equation below as an important parameter for exploiting the behavior of DASPMI molecule bound to AOT reverse micelles instead of placing too much emphasis on the magnitude of individual decay constants in such bi-exponential decays.

$$\langle t_f \rangle = a_1\tau_1 + a_2\tau_2$$

The average lifetime values are given in Table 5. The most interesting feature of our investigation with a probe having ICT state is the increase in the mean fluorescence lifetime with increased water content in the micelle.

In very low polarity solvent like heptane DASPMI shows very small ICT emission, because of such low polarity the barrier of formation of ICT from the LE state is large enough. In going from heptane to reverse micelles the polarity increases which favors the enhanced rate of the conversion from LE to ICT state so in RMs with increasing W value the ICT state is the only emitting state. The lifetime of ICT state also increases from low W value to high W value in reverse micelle. To explain this it is considered that there are two competing processes—formation of the ICT state and subsequent non-radiative decay of the ICT state. As the solvent polarity increases the rate of formation of ICT state increases. Again, with increasing solvation of the ICT state the energy gap between the ICT state and low-laying dark triplet and/or ground state decreases. According to the energy gap law of non-radiative transitions a decrease in energy gap results in an increase in the non-radiative rates, hence a decrease in the yield of the ICT state would ensue. In pure water DASPMI lifetime reduces to ~840 ps which has been attributed to the stabilized CT state accompanied by an increase in the non-radiative decay. We can calculate the radiative and non-radiative rate constants for the ICT process, from the observed φ_f and τ_f, using the following relations (1) and (2) which are more supporting and explaining the above observation.

$$K_r = \frac{\varphi_f}{\tau_f} \quad (1)$$

$$\frac{1}{\tau_f} = K_r + K_{nr} \quad (2)$$

where φ_f, τ_f, K_r and K_{nr} are the fluorescence quantum yield, mean fluorescence lifetime, radiative rate constant, and non-radiative rate constants respectively.

It may be observed from Table 3 that with the increase in W the non-radiative rate constant K_{nr} increases. We compared the non-radiative rate constant of ICT process in reverse micelles with that in pure water. The K_{nr} in water is remarkably higher than that in reverse micelles. In different RMs the variation of non-radiative rate constants for ICT process is dependent on the location of the probe [70]. The observed spectral variation of emission of DASPMI with increased hydration negates the possibility of finding the probe near n-heptane region. From the difference of the parameters (steady state fluorescence, anisotropy, fluorescence lifetime, and non-radiative rate constants) of the probe in the reverse micelles and the bulk water we can rule out the possibility of the probe staying in the core region of the micelle. So it is very logical to say that the probe molecule resides at the AOT/water interface (Scheme 1). The spectral variation of emission spectra (Table 6) in BHDC with increased hydration layer evinces that the possibility of finding the probe near core region is very thin. The fluorescence lifetime and the steady state anisotropy value (Table 6) confirm that the probe is far from the core region in the reverse micelle but it is not that far to go in n-heptane region.

Table 6
Lifetime data and anisotropy data of DASPMI in BHDC reverse micelle as a function of W.

W	Emission max (nm)	a_1	τ_1 (ps)	a_2	τ_2 (ps)	$\langle\tau_f\rangle$ (ps)	r
0	553	0.7	960	0.3	1055	989	0.064
2	552	0.7	957	0.3	1053	986	0.065
4	551	0.71	955	0.29	1054	984	0.066
6	550	0.73	956	0.27	1052	982	0.067
8	549.5	0.75	955	0.25	1051	979	0.067
10	549	0.78	956	0.22	1051	977	0.068
16	549	0.78	955	0.22	1050	976	0.069

3.9. Pico-second anisotropy decay

Fluorescence anisotropy is a property which is dependent upon rotational diffusion of the fluorophore and the fluorescence lifetime. The steady state anisotropy change of DASPMI as a function of W is not due to any change in lifetime, the rotational correlation times for DASPMI in AOT reverse micelles with increasing hydration were calculated using Perrin's equation [58]

$$\tau_c = \frac{\langle\tau_f\rangle \cdot r}{r_0 - r}$$

where $\langle\tau_f\rangle$, r, r_0 are mean fluorescence lifetime, steady state anisotropy, limiting anisotropy of DASPMI, respectively. Here as Perrin's equation is not strictly valid for heterogeneous medium we use mean fluorescence lifetime to get the approximate result. The rotational correlation time is determined from the above equation taking $r_0 = 0.38$ (from time resolved anisotropy study) with varying W. Fig. 5a shows significant decrease in rotational correlation time with W which confirms that with increasing hydration there is a decrease in rotational restriction experienced by the probe molecules.

4. Conclusion

The present work evinces that the photophysical properties of DASPMI are quite different in biomimetic reverse micelle than those in bulk water. This polarity-sensitive probe was used to determine the in situ micropolarity as well as microviscosity at the probe binding site, i.e., micellar interface as a function of micellar core size (W). This is a veritable study in locating the probe along with the orientation in cationic and anionic reverse micelles. The values of partition constants in RMs correlate well with the position of emitting probe and the affinity for the probe to enter BHDC has been explained. The knowledge of DASPMI photophysics in microenvironment gives a significant knowledge from the biological point of view to understand microheterogeneous environments like protein and allied enzymes.

References

[1] J.H. Fendler, Membrane Mimetic Chemistry, Wiley Interscience, New York, 1982, Chapter 3.
[2] P.E. Zinsli, J. Phys. Chem. 83 (1979) 3223–3231.
[3] P.L. Luisi, M. Giomini, M.P. Pileni, B.H. Robinson, Biochim. Biophys. Acta 947 (1988) 209–246.
[4] J.K. Thomas, The Chemistry of Excitation at Interfaces American Chemical Society Monograph Series 181, American Chemical Society, Washington, DC, 1984, p. 192.
[5] C. Gonzalez-Blanco, L.J. Rodriguez, M.M. Velazquez, J. Colloid Interface Sci. 211 (1999) 380–386.
[6] G. Onori, A. Santucci, J. Phys. Chem. 97 (1993) 5430–5434.
[7] J.B. Brubach, A. Mermet, A. Filabozzi, A. Gerschel, D. Lairez, M.P. Krafft, P. Roy, J. Phys. Chem. B 105 (2001) 430–435.
[8] T.K. Jain, M. Varshney, A. Maitra, J. Phys. Chem. 93 (1989) 7409–7416.

[9] J. Faeder, M.V. Albert, B.M. Ladanyi, Langmuir 19 (2003) 2514–2520.
[10] J. Faeder, B.M. Ladanyi, J. Phys. Chem. B 104 (2000) 1033–1046.
[11] J. Faeder, B.M. Ladanyi, J. Phys. Chem. B 105 (2001) 11148–11158.
[12] E.M. Corbeil, N.E. Levinger, Langmuir 19 (2003) 7264–7270.
[13] D. Pant, N.E. Levinger, Langmuir 16 (2000) 10123–10130.
[14] R.E. Riter, D.M. Willard, N.E. Levinger, J. Phys. Chem. B 102 (1998) 2705–2714.
[15] P. Hazra, N. Sarkar, Chem. Phys. Lett. 342 (2001) 303–311.
[16] D. Mandal, S.K. Pal, A. Datta, K. Bhattacharyya, Anal. Sci. 14 (1998) 199–202.
[17] A. Datta, D. Mandal, S.K. Pal, K. Bhattacharyya, J. Phys. Chem. B 101 (1997) 10221–10225.
[18] A.M. Vinogradov, A.S. Tatikolov, S.M.B. Costa, Phys. Chem. Chem. Phys. 3 (2001) 4325–4332.
[19] A. Datta, D. Mandal, S.K. Pal, K. Bhattacharyya, Chem. Phys. Lett. 278 (1997) 77–82.
[20] T. Patzlaff, M. Janich, G. Seifert, H. Graener, Chem. Phys. 261 (2000) 381–389.
[21] G. Seifert, T. Patzlaff, H. Graener, Phys. Rev. Lett. 88 (2002) 140406–147402.
[22] R.A. Marcus, Rev. Mod. Phys. 65 (1993) 599–610, and references therein.
[23] Z.R. Grabowski, Pure Appl. Chem. 65 (1993) 1751–1756.
[24] H. Lueck, M.W. Windsor, W. Rettig, J. Phys. Chem. 94 (1990) 4550–4559.
[25] B. Strehmel, H. Seifert, W. Rettig, J. Phys. Chem. B 101 (1997) 2232–2243.
[26] P. Fromherz, K.H. Dambacher, H. Ephardt, A. Lambacher, C.O. Müller, R. Eigl, H. Schaden, O. Schenk, T. Vetter, Ber. Bunsen-Ges. Phys. Chem. 95 (1991) 1333.
[27] L.M. Loew, S. Scully, L. Simpson, A.S. Waggoner, Nature 281 (1979) 497–499.
[28] R. Ramadass, J. B-Hahn, J. Phys. Chem. B 111 (2007) 7681–7690.
[29] J. Bereiter-Hahn, K.H. Seipel, M. Vöth, J.S. Ploem, Cell Biochem. Funct. 1 (1983) 147–155.
[30] B. Strehmel, W. Rettig, J. Biomed. Opt. 1 (1996) 98–109.
[31] H. Ephardt, P. Fromherz, J. Phys. Chem. 95 (1991) 6792–6797.
[32] S.P. Spooner, D.G. Whitten, in: V. Ramamurthy (Ed.), Photochemistry in Organized and Constrained Media, Wiley-VCH, Weinheim, Germany, 1991, pp. 691–739.
[33] D. Sahoo, S. Chakravorti, Phys. Chem. Chem. Phys. 10 (2008) 5890–15890.
[34] S. Panja, S. Chakravorti, Chem. Phys. Lett. 367 (2003) 330–338, and the references cited therein.
[35] M. Novaira, M.A. Biasutti, J.J. Silber, N.M. Correa, J. Phys. Chem. B 111 (2007) 748–759.
[36] P. Chowdhury, S. Panja, S. Chakravorti, J. Phys. Chem. A 107 (2003) 83–90.
[37] S. Mitra, N. Tamai, Chem. Phys. 246 (1999) 463–475.
[38] D.V. O'Connor, D. Phillips, Time-Correlated Single Photon Counting, Academic Press, New York, 1984, Chapter 6.
[39] M. Bellete^te, M. Lachapelle, G. Durocher, J. Phys. Chem. 94 (1990) 7642–7648.
[40] M. Bellete^te, G. Durocher, J. Colloid Interface Sci. 134 (1990) 289–293.
[41] J.J. Silber, M.A. Biasutti, E. Abuin, E. Lissi, Adv. Colloid Interface Sci. 82 (1999) 189–252.
[42] M. Ueda, Z.A. Schelly, Langmuir 5 (1989) 1005–1008.
[43] E. Lissi, E. Abuin, in: S.D. Christian, J.F. Scamehorn (Eds.), Solubilization in Surfactant Aggregates, Marcel Dekker, New York, 1995.
[44] R.D. Falcone, N.M. Correa, M.A. Biasutti, J.J. Silber, J. Colloid Interface Sci. 296 (2006) 356–364.
[45] J.R. Lakowicz, Principles of Fluorescence Spectroscopy, 2nd ed., Kluwer Academic, New York, 1999.
[46] M. Wang, J.K. Thomas, M. Gratzel, J. Am. Chem. Soc. 98 (1976) 2391–2397.
[47] J. Guharay, P.K. Sengupta, Chem. Phys. Lett. 75 (1994) 230–233.
[48] Devaki A. Kelker, A. Chattopadhyay, J. Phys. Chem. B 108 (2004) 12151–12158.
[49] A. Morimoto, T. Yatsuhashi, T. Shimada, S. Kumazaki, K. Yoshihara, H. Inoue, J. Phys. Chem. A 105 (2001) 8840–8849.
[50] P.R. Bangal, S. Panja, S. Chakravorti, J. Photochem. Photobiol. A: Chem. 139 (2001) 5–16.
[51] W.M. Kwok, M.W. George, D.C. Grills, C. Ma, P. Matousek, A.W. Parker, D. Phillips, W.T. Toner, M. Towrie, Angew. Chem. Int. Ed. Engl. 42 (2003) 1826–1830.
[52] N. Sarkar, K. Das, A. Datta, S. Das, K. Bhattacharya, J. Phys. Chem. 100 (1996) 10523–10527.
[53] A. Mallick, S.C. Bera, S. Maiti, N. Chattopadhyay, Biophys. Chem. 112 (2004) 9–14.
[54] B. Sengupta, P.K. Sengupta, Biochem. Biophys. Res. Commun. 277 (2000) 13–19.
[55] R.B. Macgregor, G. Weber, Nature 319 (1986) 70–73.
[56] C. Reichardt, in: H. Ratajazak, W.J. Orville-Thomas (Eds.), Molecular Interaction, vol. 3, Wiley, New York, 1982, p. 255.
[57] M. Novaria, F. Moyano, M.A. Biasuuti, J.J. Silber, N.M. Correa, Langmuir 24 (2008) 4637–4646.
[58] J.R. Lakowicz, Principles of Fluorescence Spectroscopy, Plenum, New York, 1983.
[59] X. Wang, J. Wang, Y. Wang, H. Yan, P. Li, R.K. Thomas, Langmuir 20 (2004) 53–56.
[60] T.K. Jain, M. Varshey, A. Maitra, J. Phys. Chem. 93 (1989) 7409–7416.
[61] S.M. Andrade, S.M.B. Costa, R. Pansu, Photochem. Photobiol. 71 (2000) 405–412.
[62] M. Moran, G.A. Bowmaker, R.P. Cooney, Langmuir 11 (1995) 738–743.
[63] M. Panda, P.K. Behera, B.K. Misra, G.B. Behera, J. Photochem. Photobiol. A 90 (1995) 69–73.
[64] J. Eastoe, T.F. Towey, B.H. Robinson, J. Williams, R.K. Heenan, J. Phys. Chem. 97 (1993) 1459–1463.
[65] S.A.P. Goncalves, S.H. De Pauli, A.C. Tedesco, F.H. Quina, L.T. Okano, J.B.S. Bhnilha, J. Colloid Interface Sci. 267 (2003) 494–499.
[66] F.G. Prendergast, Curr. Opin. Struct. Biol. 1 (1991) 1054–1059.
[67] A. Chattopadhyay, S. Mukherjee, H. Raghuraman, J. Phys. Chem. B 106 (2002) 13002–13009.
[68] C.H. Cho, M. Chung, J. Lee, T. Nguyen, S. Singh, M. Vedamulthu, S. Yao, S.B. Zhu, G.W. Robinson, J. Phys. Chem. 99 (1995) 7806–7812.
[69] D. Torphin, J. Svodova, I. Konopasek, L.J. Brand, J. Chem. Phys. 96 (1992) 7919–7930.
[70] P. Hazra, D. Chakraborty, N. Sarkar, Langmuir 18 (2002) 7872–7879.